Numerical Methods in Civil Engineering, 10-2 (2025) 60-70

Numerical Methods in Civil Engineering

Journal Homepage: https://nmce.kntu.ac.ir/

Predicting post-earthquake fire behaviour of steel moment frames using different classification models

Parviz Ahadi*, Kazem Shakeri, Vahid Akrami****

ARTICLE INFO

RESEARCH PAPER

Article history:
Received:
December 2025
Revised:
January 2026
Accepted:
February 2026

Keywords:
Steel Frame Structures
Fire loading
Seismic hazard
Numerical Simulation
Data-Driven Approach

Abstract:

Post-earthquake fire (PEF), often triggered by damage to electrical and gas systems, poses a severe threat to steel structures, especially when seismic damage disables fire protection systems. Accurately predicting structural behavior under PEF is critical for emergency response. This study investigates the behavior of steel Moment-Resisting Frames (MRFs) under PEF through a two-phase approach. In the first phase, finite element (FE) simulations of 4- and 8-story intermediate and special MRFs were conducted under various fire scenarios (single-bay, two-bay, and entire-floor) following different seismic intensity levels (without earthquake, with design base earthquake and with maximum considered earthquake). Then the structural response of different models was investigated and compared in terms of failure modes (local, partial, global) and fire resistance times, revealing significant insights into the combined effects of building height, frame type, fire location, and prior seismic damage. In the second phase, the study employs Machine Learning (ML) techniques to predict the stability of steel MRFs under PEF. Using the dataset generated from FE simulations, five common ML models were trained and tested. The results demonstrate that ML techniques are highly effective tools for predicting both the failure mode and collapse time of steel MRFs subjected to PEF, providing a rapid assessment methodology that complements detailed numerical analysis for emergency response scenarios.

1. Introduction

Earthquakes frequently trigger secondary disasters, with post-earthquake fire (PEF) being a major threat due to damage to electrical and gas infrastructure. The initial seismic event can induce residual drifts, which critically compromise a structure's resistance to subsequent fire by damaging active and passive fire protection systems [1]. The intrinsic complexity of PEF scenarios, involving varying seismic intensities, complex fire dynamics, and force redistribution after member failure, makes it exceptionally challenging to develop a generic analytical method for predicting structural robustness [2].

* *Faculty Member, Department of Civil Engineering, Germi Branch, Islamic Azad University, Germi, Iran.*
** *Professor, Faculty of Engineering, University of Mohaghegh Ardabili, Ardabil, Iran.*
*** *Corresponding author: Associate Professor, Faculty of Engineering, University of Mohaghegh Ardabili, Ardabil, Iran. v.akrami@uma.ac.ir*

When compared to systems like braced frames or steel plate shear walls, which rely on a primary load-resisting element, the post-earthquake fire performance can diverge significantly [3, 4]. MRFs benefit from greater redundancy and moment-redistribution capacity [5, 6], whereas systems with a dominant lateral-load element may be more susceptible to a rapid loss of global stability if that element is both seismically damaged and thermally weakened [3, 4]. However, the greater ductility of moment-resisting frames can also lead to larger residual drifts, potentially making them more vulnerable to post-earthquake fire [5, 6]. Given these complexities, understanding the performance of steel structures under such multi-hazard conditions is vital. Steel moment-resisting frames (MRFs) are inherently vulnerable under fire conditions alone, a concern underscored by research focused solely on thermal loading [7, 8]. For instance, Shakeri et al. [9] and Miryousefi et al. [10]

https://doi.org/10.61882/NMCE.2512.1112

demonstrated that, depending on key design parameters such as ductility class, building height, and the level of applied gravity loads, exposure to fire can lead to structural collapse. Also, Behnam [11] demonstrated that the vulnerability of structures designed for progressive collapse under combined column loss and localized fire is highly sensitive to structural configuration and the vertical location of the fire. This inherent vulnerability is critically exacerbated when fire follows an earthquake. Existing research on the post-earthquake fire resistance of steel MRFs presents a complex and sometimes contradictory picture. Several studies, such as those by Behnam & Ronagh [5], Zhou et al. [12] and Ahadi et al. [6], have conclusively demonstrated that prior earthquake damage significantly reduces fire resistance. This is further supported by Erfani & Dehestani [13], who showed the drastic reduction in the fire-resistance of damaged connections. Risco et al. [14] demonstrated that residual drifts may cause a significant reduction in fire resistance for protected frames due to damage to the fireproofing material, which alters the collapse mode of the structure. Other studies [15] have shown that while earthquake damage might not universally increase the probability of reaching performance limit states under fire, it can critically redistribute demands and induce instability in perimeter columns during a PEF. A recent comprehensive review by Dashti et al. [16] consolidates these findings, confirming that seismic damage critically degrades fire resistance. However, other researchers like Suwondo et al. [17] and Alasiri et al. [18] have reported that residual seismic deformations had a negligible influence on the ultimate collapse mechanism, suggesting that gravity systems govern the final response. This discrepancy, also noted in studies like Alisawi et al. [19], underscores the highly non-linear and system-dependent nature of PEF performance. Alongside these investigations, probabilistic frameworks have been developed to assess structural vulnerability under multi-hazard scenarios. For instance, fragility functions have been created specifically for PEF in braced frames [4] and, more broadly, for fire scenarios in steel buildings [20, 21], linking hazard intensity measures to the probability of structural failure.

Concurrently, Machine Learning (ML) techniques have emerged as a powerful paradigm for solving complex engineering problems [22] where traditional theoretical models are intractable, as noted by early adopters in structural mechanics [23]. A review by Kürüm Varolgüneş and Varolgüneş [24] has identified the ML techniques as appropriate tools for multi-hazard resilience assessment of structures subjected to PEF. The success of these techniques is evident in recent fire safety applications [25]. For instance, Fu [26] applied ML to assess fire-induced progressive collapse, and Ye & Hsu [27] used it for real-time deformation prediction of steel structures in fire. Similarly, Zhu et al. [28] demonstrated ML's efficacy in assessing the dynamic progressive collapse of steel frames. Also, Harati and van de Lindt [29] successfully employed an ML synthesis framework to generate accurate fragility surfaces for steel MRFs under PEF.

Despite these advancements, critical gaps remain in both understanding the combined influence of key design parameters on the PEF behaviour of steel MRFs and in predicting their failure mode and collapse time using fast and accurate methods. To address these gaps, this study first quantifies the effects of seismic intensity, frame type, height, and fire location on failure mechanisms through comprehensive FE analysis. Then, it develops and compares efficient ML models capable of instantaneously predicting both failure mode and collapse time, thereby bridging the critical gap between detailed simulation and urgent decision-making needs. Consequently, this study employs an integrated two-phase methodology to investigate steel MRFs under PEF (**Fig. 1**).

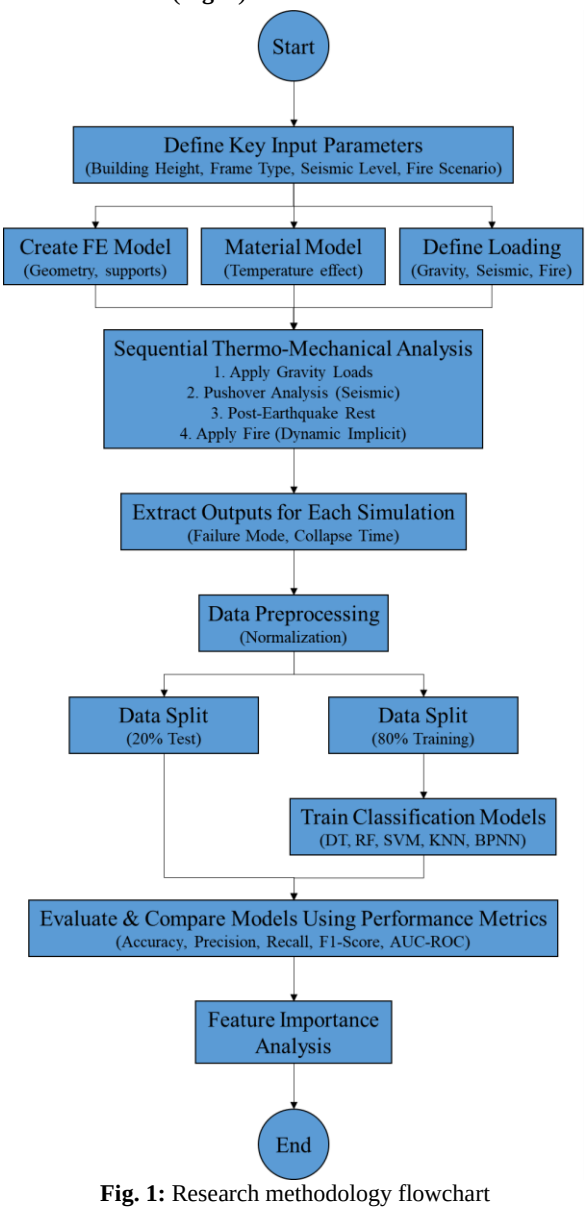

Fig. 1: Research methodology flowchart

The first phase utilizes finite element simulations of 4- and 8-story intermediate and special MRFs under various post-earthquake fire scenarios to analyze failure modes and resistance times, revealing critical insights into the combined effects of building height, frame type, and fire location. Given that seismic damage can compromise the integrity of fire protection materials as demonstrated by Behnam & Abolghasemi [30], the present analyses focus on the inherent resistance of the structural steel frame by excluding fireproofing from the models. The second phase uses this dataset to train and test five ML models, demonstrating their high effectiveness in predicting both failure mode and collapse time, thereby providing a rapid assessment tool that complements traditional numerical analysis for post-earthquake emergency response.

2. MATERIALS AND PROCEDURES

This study employs a machine learning (ML) model to assess the post-earthquake fire resistance of steel MRFs. The general framework (as shown in **Fig. 1**), comprises three main stages: I) data generation, II) ML model development, and III) predictive model application. The data generation is the central part of the procedure and involves three sub-stages. First, a Python script generates Finite Element (FE) models based on frame type (Intermediate or Special) and the number of stories (4 or 8), assigning temperature-dependent material properties. The schematic configurations of the 4- and 8-story prototype buildings are shown in **Fig. 2** and **Fig. 3**. Second, the loading conditions are defined, including gravity loads (dead: 5.45 kN/m^2, Live: 2.5 kN/m^2), seismic loads (no earthquake, design base earthquake (DBE), and maximum considered earthquake (MCE) as per **Table 1**), and various fire scenarios (single-bay, multi-bay, or entire floor scenarios). Third, a heat transfer analysis is conducted on members in the burning bays to provide temperature histories for the subsequent structural analysis.

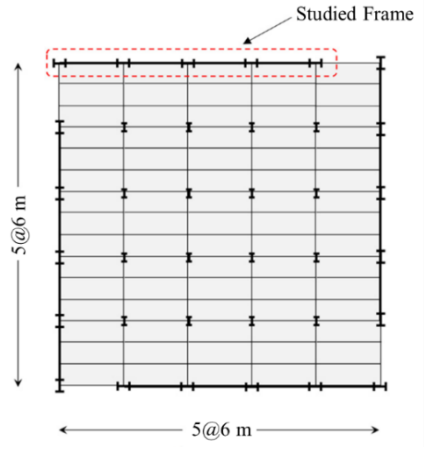

Fig. 2: Plan view of the studied frames

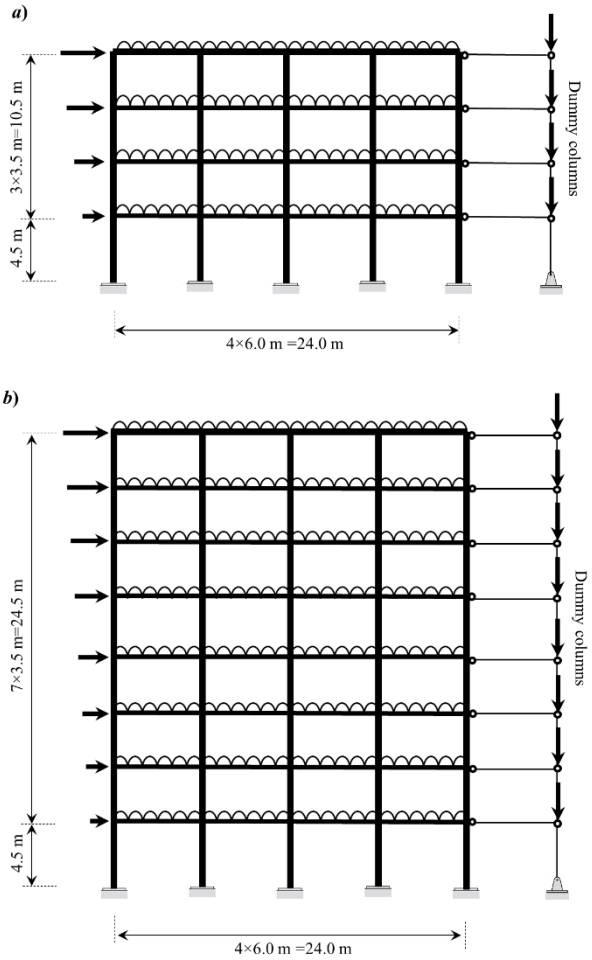

Fig. 3: Elevation view of the 4-story and 8-story frames

Table 1: DBE and MCE target displacements

Model	Intermediate moment frame	Special moment frame
4 story	δ_{DBE}=0.26 δ_{MCE}=0.39	δ_{DBE}=0.33 δ_{MCE}=0.49
8 story	δ_{DBE}=0.41 δ_{MCE}=0.62	δ_{DBE}=0.50 δ_{MCE}=0.75

The core of data generation is the FE modeling, which uses ABAQUS [31] via a Python script to perform a sequential thermo-mechanical analysis. The process involves: 1) applying gravity loads, 2) performing a pushover analysis for seismic loading, 3) simulating a post-earthquake state of rest, and 4) applying temperature effects in a dynamic implicit analysis based on a selected fire scenario (fire story, bay and width). The structural model uses B31 beam elements with steel material (Young's modulus of 210 GPa, yield stress of 340 MPa, and Poisson's ratio of 0.3). The degradation of these mechanical properties at elevated temperatures was modeled using the reduction factors prescribed by Eurocode 3 [32], as detailed in **Fig. 4**. A critical part of this process is the uncoupled heat transfer analysis (shown in **Fig. 5**), which uses DC3D8 thermal elements to solve the three-dimensional conduction problem and

determine the temperature distribution within the structural elements prior to the mechanical response. The thermal properties of steel (conductivity, specific heat, and density) were based on Memari et al. [33]. The ISO 834 [34] standard fire curve was applied as the prescribed thermal boundary condition to the elements based on the selected fire scenario. This curve was selected as a conservative and standardized benchmark to ensure a consistent and comparable assessment of structural performance across all analyzed scenarios. Its use allows the effects of earthquake-induced damage to be isolated from uncertainties associated with fire development, while maintaining consistency with established design codes and previous PEF studies. To evaluate both localized and global structural response, a range of fire scenarios was modeled, including single-bay, two-bay (adjacent), and whole-floor (extreme) fires. The fire exposure was modeled realistically to account for member type and location. In this regard, interior columns in fully involved bays were exposed to fire on all four sides, while exterior columns, interior columns in single-bay fires, and all beam elements (considering the shielding effect of a concrete slab) were exposed on three sides only [33].

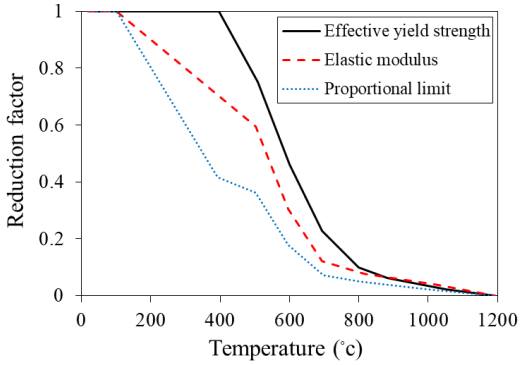

Fig. 4: Material properties degradation with temperature according to Eurocode 3 [32]

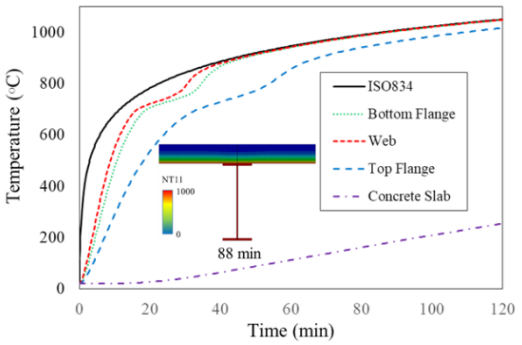

Fig. 5: An example of heat transfer analysis for a beam element

The accuracy of the coupled numerical model was validated by modeling a two-span, single-story frame tested by Robert and Schaumann [35, 36]. For this validation model, IPE80 I-sections were used for both beams and columns, with each column supporting a gravity load of 74 kN and the structure subjected to a total lateral load of 2.85 kN. A fire load was applied to the left bay of the frame. The comparison of results, presented in **Fig. 6**, shows strong agreement with existing experimental and numerical data, confirming the model's reliability.

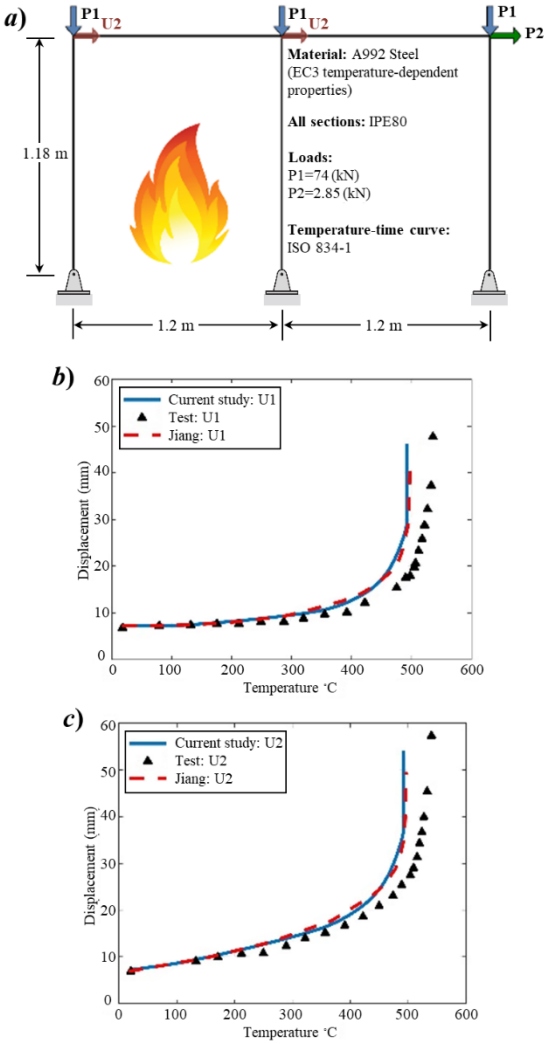

Fig. 6: FE model validation; a) modelled frame; b) horizontal displacement at the top of left column (U1); c) horizontal displacement at the top of middle column (U2)

3. RESULTS OF FIRE ANALYSES

3.1. Overall Performance and Failure Modes

This section presents a general overview of the structural performance and failure modes observed in the analyzed intermediate and special moment frames subjected to various fire scenarios, including post-earthquake fire events. In general, the structural response to fire, whether in intact structures or those pre-damaged by an earthquake, is a dynamic process of load redistribution. As the temperature rises in the fire-affected compartment, the affected steel members gradually lose their strength and stiffness. This forces the gravitational loads to be redistributed to adjacent

cooler members, creating alternative load paths. The stability of the structure ultimately depends on the ability of these alternative paths to withstand the redistributed loads. If the surrounding frame possesses sufficient capacity and redundancy, deformations stabilize, and the structure survives. Conversely, if the alternative load paths are inadequate, deformations increase progressively, leading to structural collapse. Accordingly, the structural responses observed in the analyses were categorized into three distinct failure modes based on the extent of damage and its impact on global stability (see **Fig. 7**). These classifications are defined as follows:

- **Local Failure (L):** This type of failure is characterized by the excessive deformation or rupture of individual beam elements within the fire-affected compartment, exceeding the predefined deflection limits of L/20 or $L^2/400d$ (L and d, represent the clear span length and overall depth of the beam, respectively). Crucially, in this mode, the lateral inter-story drift remains below the 0.1 rad threshold, the structure's lateral load-bearing system remains largely intact, and no progressive collapse mechanism is triggered. This was the most prevalent outcome for single-bay fire scenarios.
- **Partial Failure (P):** This type of failure involves a more severe level of damage where the failure propagates beyond a single beam to include the buckling of one or more columns in the fire-affected bay. This leads to the collapse of that specific structural portion but does not result in the collapse of the entire frame. This mode is identified by a lateral story drift that surpasses 0.1 rad with a sharp, near-vertical slope in the drift-time history. Partial failures were typically observed in top-story, edge-bay scenarios, where the structural redundancy is lower.
- **Global Failure (G):** This type of failure represents the most severe case, where the loss of key structural elements initiates a progressive collapse. In this mode, the vertical load path is completely severed, leading to global instability. The defining indicator is a lateral story drift exceeding 0.1 rad across multiple stories, signifying that the structure can no longer redistribute loads and has lost its overall integrity. This failure mode occurred consistently and exclusively under entire floor fire scenarios.

The fire resistance time for each scenario was defined as the time from the start of fire exposure until the first occurrence of any failure mode, whichever happened sooner. According to the results, the spatial distribution of the fire was the primary factor governing both the failure mode and the fire resistance time (see **Table 2** & **Table 3**). Single-bay fires predominantly resulted in local failures, allowing the structure to achieve significantly longer fire resistance times, often exceeding 45-100 minutes, as the load was successfully redistributed.

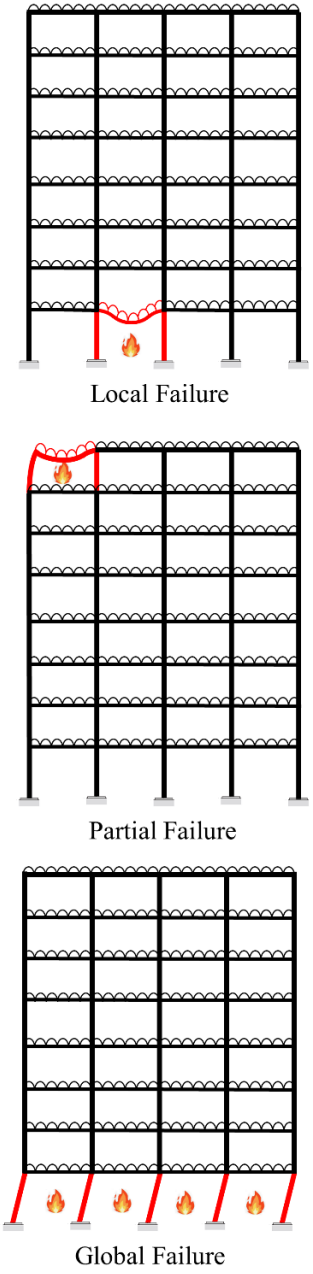

Fig. 7: Different failure modes in analyzed models

Table 2: Failure mode occurrence rates for different fire scenarios

Fire scenario	Local Failure	Partial Failure	Global Failure
Single-bay fire	87.8%	12.2%	0%
Two-bay fire	46.8%	11.1%	42.1%
Entire floor fire	0%	0%	100%

Table 3: Average failure times for different fire scenarios (min)

Fire scenario	Local Failure	Partial Failure	Global Failure
Single-bay fire	70.9 ± 27.9	35.3 ± 9.2	-
Two-bay fire	51.3 ± 16.2	33.3 ± 8.0	42.9 ± 9.5
Entire floor fire	-	-	30.5 ± 10.1

In contrast, entire floor fires consistently led to rapid global collapse, drastically reducing the resistance time to as low as

20-40 minutes in critical scenarios, as the widespread loss of member capacity eliminated alternative load paths. Having established the fundamental behavioral patterns of the analyzed models, the subsequent sections provide a detailed comparative analysis of the effects of building height and frame type on specific performance indicators such as fire resistance time and failure mode.

3.2. Comparison of Low- and Mid-Rise Frames

The comparison of models with different numbers of stories reveals a significant influence of building height on failure mode distribution. **Fig. 8** displays the effect of building height on structural performance under fire loading. As shown in **Fig. 8**(a), the taller frames demonstrated better performance with increased local failures and decreased partial failures, indicating the positive effect of increased structural redundancy in containing failure progression. The proportion of global failures remained relatively similar between both heights, suggesting that the building height has a limited influence on the global failure mode. Fire resistance time for different number of stories and failure modes is demonstrated in **Fig. 8**(b). According to the figure, the taller frames exhibited significantly longer resistance in local failure scenarios, demonstrating 38% improvement compared to the low-rise frames. In the partial failure mode, the resistance time increased by 12.6%, while for global failures, the time remained almost similar for both frame heights.

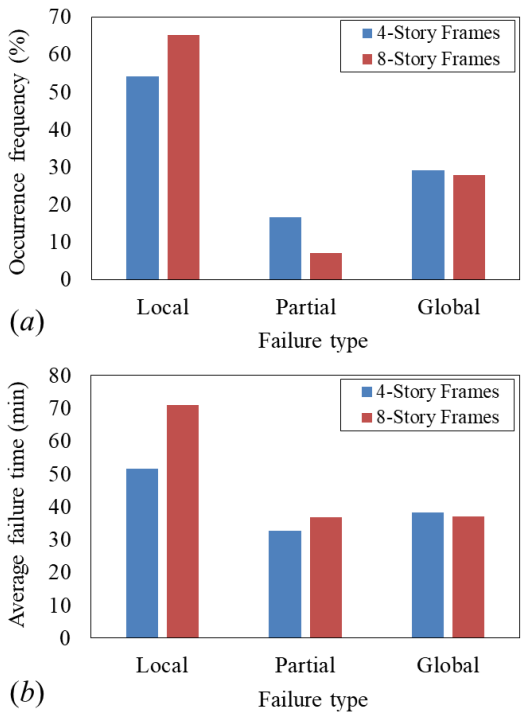

Fig. 8: The effect of building height on structural performance: (a) distribution of failure modes; (b) fire resistance time for different failure modes.

The influence of fire location within the building height was subsequently investigated, as presented in **Fig. 9**. The variation of failure mode frequency with normalized height of burning story is presented in **Fig. 9**(a). It can be observed that upper-story fires produced the highest proportion of partial failures, while reducing the occurrence of local and global failures. This suggests that fire elevation plays a critical role in determining the failure mechanism. **Fig. 9**(b) demonstrates the average failure time as a function of normalized height and fire type. The results indicate that single-bay fires in upper levels have less resistance time compared to fires in lower levels. In contrast, entire floor fires exhibit minimal sensitivity to vertical location, demonstrating consistent collapse behavior regardless of fire elevation within the structure.

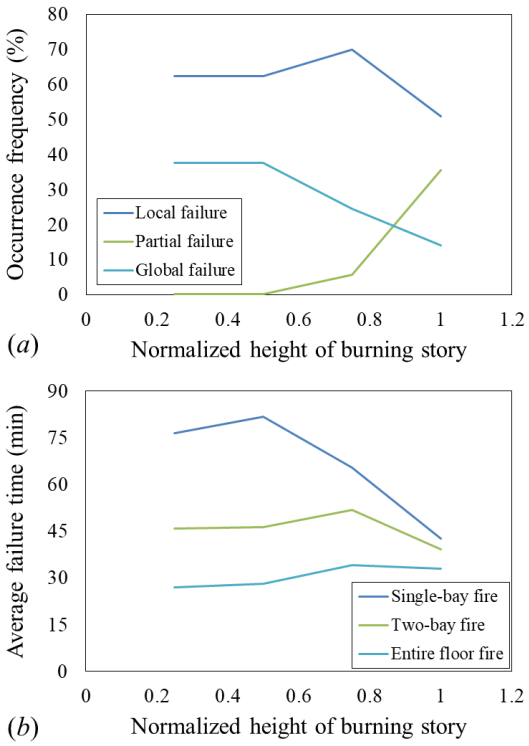

Fig. 9: The influence of fire elevation on structural behavior: (a) failure mode occurrence versus normalized height; (b) collapse time versus normalized height and fire type.

3.3. Effect of Frame Type and Seismic Level

Comparing results for different frame types shows distinct behavioral patterns between intermediate and special moment frames. As shown in **Table 4**, intermediate frames exhibited a higher occurrence of local failures and lower rates of global failures compared to special frames. The primary reason for this behavior can be attributed to the greater resistance and stiffness of intermediate frame sections, which enables them to better withstand stress redistribution during fire exposure, thereby holding damage at the local level and preventing its progression to global collapse. **Table 5** demonstrates that this advantage in failure mode distribution is linked to the longer fire resistance times

for intermediate frames across all failure modes. Specifically, intermediate frames showed almost 40% longer resistance in local and partial failure scenarios, and 10% longer in global failures.

Table 4: Failure mode occurrence rates for different frame types

Frame type	Local Failure	Partial Failure	Global Failure
Intermediate	63.5%	9.7%	26.7%
Special	59.4%	10.8%	29.9%

Table 5: Average failure times across different frame types

Fire scenario	Local Failure	Partial Failure	Global Failure
Intermediate	75.9 ± 26.2	40.8 ± 8.7	39.3 ± 13.0
Special	54.0 ± 21.9	28.8 ± 2.8	35.8 ± 9.9

The influence of prior seismic damage on structural fire resistance of the models is presented in **Fig. 10**(a) and (b), which display failure mode distribution and fire resistance times across different seismic levels, respectively. **Fig. 10**(a) shows a clear trend of progressive deterioration in structural resilience with increasing seismic intensity. As the seismic level escalates from fire-only to post-MCE conditions, the occurrence of local failures decreases while both partial and global failures show consistent increases. This pattern indicates that pre-existing seismic damage reduces the structure's ability to sustain fire induced redistribution of forces.

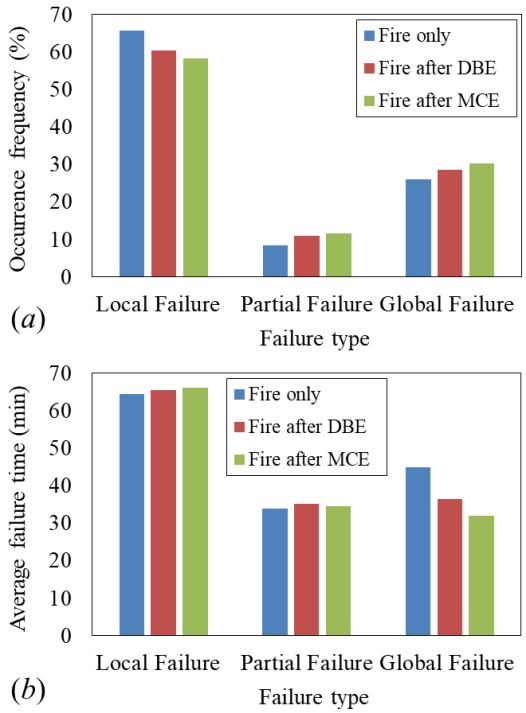

Fig. 10: The effect of prior seismic level on structural performance under fir e: (a) failure mode occurrence rates; (b) average fire resistance times

Fig. 10(b) provides further insight into this degradation mechanism by examining the fire resistance time. Interestingly, while local and partial failure times remain relatively stable across seismic levels, the global failure mode exhibits significant sensitivity to prior damage. The global failure mode resistance time demonstrates a 28.7% decrease from fire-only conditions to fire following MCE-level earthquakes. This pronounced reduction in global failure resistance underscores the critical importance of considering cumulative damage effects in performance-based design, as the combined action of seismic and fire loading fundamentally alters the collapse behavior and significantly compromises structural endurance.

4. ML MODEL DEVELOPMENT

4.1. Feature Indices and Target Variables

The development of the machine learning model involved defining the key input parameters and output responses that characterize the structural behavior under post-earthquake fire. Five primary input parameters were selected to effectively capture the critical aspects of the scenario. These include:

- The number of stories,
- Frame type (categorized as Intermediate or Special Moment Frames),
- The fire type and earthquake intensity (classified as "fire only," "fire following DBE," or "fire following MCE").
- Fire width,
- Fire horizontal position, and
- Fire vertical position within the structure.

The level of seismic intensity was included as a key input feature, specifically categorized into three discrete levels: no earthquake, DBE, and MCE. All these inputs were normalized to a scale between 0 and 1 to ensure consistent model training. The ML model was configured to predict two key target variables that directly quantify the structural collapse limit state. The first target is the failure mode, formulated as a multi-class classification problem to distinguish between the three distinct collapse mechanisms established in Section 3 (i.e. local failure characterized by isolated beam failure, partial failure involving limited collapse with maintained global stability, and global failure indicating complete structural collapse). A schematic representation of these failure mode classifications is provided in Fig. 7. The second target variable is the failure time, treated as the minimum time at which any of the three failure modes (local, partial, or global) first occurred in a simulation. For the purpose of classification, this continuous time variable was discretized into four 30-minute intervals: 0–30 min, 30–60 min, 60–90 min, and 90–120 min.

4.2. Adopted ML Algorithms and Hyperparameters

To build the predictive framework, five distinct machine learning algorithms were implemented and evaluated, as schematically shown in **Fig. 11** and explained below:

- **Decision Tree (DT):** This model was selected for its interpretability and ability to model non-linear decision boundaries through a simple tree structure. Key hyperparameters included a maximum tree depth of 10 (controlled by setting the maximum number of splits), a minimum of 10 samples required to split a node, and the Gini impurity criterion for splitting.
- **Random Forest (RF):** This ensemble method was employed to improve predictive accuracy and robustness by aggregating predictions from multiple de-correlated decision trees. The model was configured with 100 trees and other hyperparameters for growing each individual tree were kept consistent with those used for DT.
- **Support Vector Machine (SVM):** This model was utilized for its effectiveness in high-dimensional spaces, using various kernel functions to find optimal separation hyperplanes. A 3rd-order polynomial kernel was used, with the regularization parameter and the kernel scale coefficient set to 1.0.

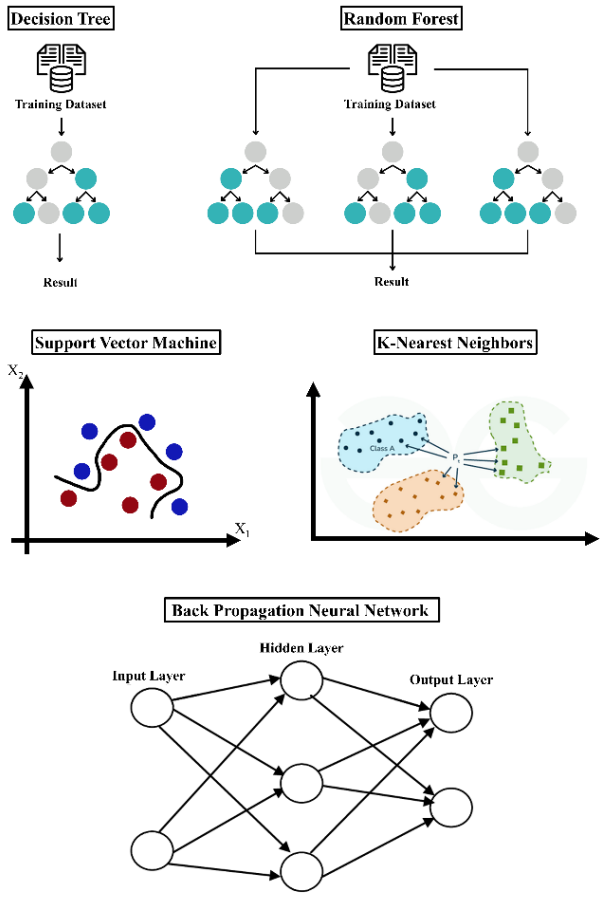

Fig. 11: Adopted machine learning algorithms

- **K-Nearest Neighbor (KNN):** This model classifies samples based on the majority class of their closest neighbors in the feature space. The number of neighbors was set to 5, using the Euclidean distance metric and uniform weighting.
- **Back Propagation Neural Network (BPNN):** BPNNs are configured to capture complex non-linear relationships through their interconnected layered architecture. This model was selected based on its capability to learn intricate patterns between input features and structural responses. The network consisted of one hidden layer with 15 neurons, using the sigmoid activation function. It was trained for 1000 epochs, optimized using the Levenberg-Marquardt backpropagation algorithm.

The dataset was split into training and testing subsets, with 80% of the data used for model training and the remaining 20% reserved for final evaluation.

4.3. Performance metrics

To assess the performance of the adopted ML models in predicting both failure type and failure time window, five key metrics were employed as defined in the following equations:

$$\text{Precision} = \frac{\text{True Positive}}{\text{True Positive} + \text{False Positive}} \quad (1)$$

$$\text{Recall} = \frac{\text{True Positive}}{\text{True Positive} + \text{False Negative}} \quad (2)$$

$$\text{F1} - \text{score} = \frac{2 \times \text{Precision} \times \text{Recall}}{\text{Precision} + \text{Recall}} \quad (3)$$

$$\text{False Positive Rat} = \frac{\text{False Positive}}{\text{False Positive} + \text{True Negative}} \quad (4)$$

The area under the receiver operating characteristic curve (AUC-ROC) was also used to evaluate the model's ability to distinguish between classes.

4.4. Model Performance Evaluation

The predictive performance of the five ML algorithms was evaluated (Fig. 12) and detailed performance metrics for both predictive models (i.e. failure type and time), are summarized in **Table 6** and **Table 7**. To assess the validity and robustness of the machine learning results, the training and testing procedure was repeated five times using independent random splits of 80% for training and 20% for testing. In each run, the complete model training and evaluation process was conducted independently, and performance metrics were computed based on the corresponding test set. The reported performance metrics represent the average values over the five runs, reducing the sensitivity of the results to a single data partition.

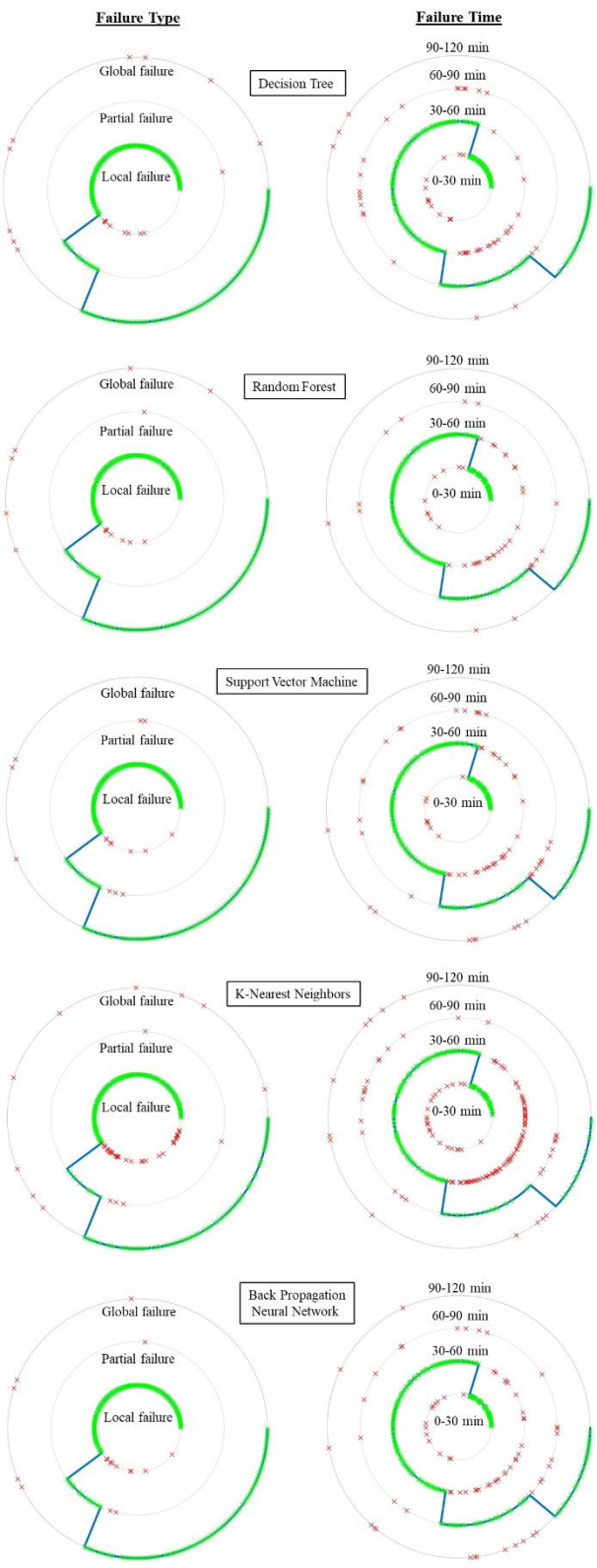

Fig. 12: Target and predicted classes for test set (blue: target class, green: correct prediction, red: wrong prediction)

According to the table, the DT model, known for its interpretable tree-like structure, demonstrated strong predictive capabilities, achieving 94.85% accuracy for failure type classification and 84.28% accuracy for failure time prediction. Furthermore, the RF algorithm, which operates as an ensemble of multiple decision trees, showed improved performance with 95.66% accuracy for failure type and 86.18% for failure time when utilizing 100 trees. In contrast to these tree-based methods, the SVM model with a 3rd-order polynomial kernel achieved the highest accuracy in failure type prediction at 96.48%, while attaining 81.84% accuracy for failure time. Meanwhile, the KNN algorithm, a distance-based method, performed competitively for failure type prediction (86.99% with five neighbors) but showed limitations in failure time estimation (66.40%). Finally, a BPNN with one layer of 15 hidden neurons achieved balanced performance with 94.58% accuracy for failure type and 81.84% for failure time.

Table 6: Performance metrics for failure type (%)

ML model	DT	RF	SVM	KNN	BPNN
Accuracy	94.85	95.66	96.48	86.99	94.58
Precision	95.36	96.01	95.19	83.21	94.21
Recall	91.72	92.18	93.63	71.6	90.66
F1-score	92.78	93.41	93.78	74.68	92.1
AUC-ROC	94.16	94.6	95.74	81.14	93.48

Table 7: Performance metrics for failure time (%)

ML model	DT	RF	SVM	KNN	BPNN
Accuracy	84.28	86.18	81.84	66.4	81.84
Precision	83.86	86.72	81.17	63.12	80.76
Recall	84.55	82.76	78.51	57.62	78.23
F1-score	82.97	83.63	78.28	58.2	78.14
AUC-ROC	89.27	88.55	85.76	71.83	85.57

4.5. Feature Importance Analysis

To identify the most influential parameters governing structural behavior under post-earthquake fire scenarios, a comprehensive feature importance analysis was conducted. Results of feature importance analysis for different predictive models are summarized in **Table 8** and **Table 9**. Across all models, feature importance analysis consistently identified fire characteristics as the most significant predictors. For failure type prediction, fire width emerged as the dominant factor, while for failure time prediction, both fire vertical position and structural parameters including building height and frame type were identified as critical determinants. The performance metrics, including precision, recall, F1-scores, and AUC-ROC values, confirmed the robustness of the implemented models, with the ensemble method (RF) and kernel-based approach (SVM) demonstrating particular effectiveness in handling the complex relationships between input parameters and structural responses under multi-hazard conditions.

Table 8: Relative importance of different parameters in failure type prediction model (%)

ML model	DT	RF	SVM	KNN	BPNN
Structural height	3	11	8	13	3
Fire type	1	5	9	6	3
Framing type	1	6	4	10	5
Fire width	100	100	100	100	100
Fire horizontal position	29	100	68	97	62
Fire vertical position	42	67	49	30	39

Table 9: Relative importance of different parameters in failure time prediction model (%)

ML model	DT	RF	SVM	KNN	BPNN
Structural height	28	53	48	23	46
Fire type	22	11	21	33	15
Framing type	58	62	48	36	38
Fire width	43	100	100	100	100
Fire horizontal position	4	2	4	13	9
Fire vertical position	100	88	80	66	82

5. CONCLUSIONS

This study investigated the behavior of steel MRFs under PEF through integrated FE and ML approaches. The results of FE analysis revealed that intermediate MRFs generally exhibited better fire resistance compared to special MRFs, achieving longer failure times across all failure modes. Also, it was shown that building height significantly influenced failure mode, with taller frames demonstrating a higher prevalence of local failures due to increased redundancy. The spatial characteristics of the fire, particularly in upper-story edge bays, were identified as critical factors leading to partial failures, while entire floor fires consistently resulted in global collapse.

Utilizing FE results, a comprehensive dataset was generated to develop an ML framework for rapid robustness assessment. Among the five ML algorithms tested, the Random Forest model demonstrated superior accuracy in predicting both failure type and collapse time. Feature importance analysis confirmed that fire characteristics, particularly fire width and vertical position, were the most significant predictors of structural response, consistent with the parametric study findings. The results conclusively highlight the potential of ML as an effective and efficient tool for multi-hazard assessment of steel structures, providing valuable insights for performance-based design and emergency response planning in PEF scenarios. The findings are particularly applicable to the preliminary evaluation and rapid screening of steel moment-resisting frame buildings subjected to standard fire exposure, supporting post-earthquake decision making and prioritization. While the developed models are specific to the structural configurations and fire scenarios considered in this study, the proposed framework can be extended to other systems and fire conditions through appropriate retraining and calibration.

REFERENCES

[1] Moradi, M., Tavakoli, H. R., & Abdollahzadeh, G. R. (2021). Comparison of steel and reinforced concrete frames' durability under fire and post-earthquake fire scenario. Civil Engineering Infrastructures Journal, 54(1), 145-168.

[2] Covi, P., Tondini, N., Korzen, M., & Tornaghi, M. L. (2025). Hybrid fire following earthquake testing of a steel braced frame. Construction and Building Materials, 496, 143731.

[3] Benvidi, A., Mohammadi Dehcheshmeh, E., Safari, P., Broujerdian, V., & Huang, S. S. (2023). Post-fire seismic performance of low-yielding-steel plate shear wall systems. International Journal of Civil Engineering, 21(10), 1661-1678.

[4] Covi, P., Tondini, N., Sarreshtehdari, A., & Elhami-Khorasani, N. (2024). Fires following earthquake fragility functions for protected steel braced frames. Fire Technology, 60(4), 2815-2844.

[5] Behnam, B., & Ronagh, H. R. (2015). Post-Earthquake Fire performance-based behavior of unprotected moment resisting 2D steel frames. KSCE Journal of Civil Engineering, 19(1), 274-284.

[6] Ahadi, P., Shakeri, K., & Akrami, V. (2022). Multi-hazard robustness of special and intermediate moment frames due to earthquake and fire. Ingegneria Sismica, 39(3), 67-87.

[7] Fanaie, N., & Razavi, M. (2022). Investigation of the performance of self-centering steel plate shear walls under fire loading. Numerical Methods in Civil Engineering, 6(4), 67-77.

[8] Pournosrat, A., Abbaszadeh, A., & Yahyai, M. (2022). Numerical investigation of the behavior of HSC columns in fire. Numerical Methods in Civil Engineering, 7(2), 61-67.

[9] Shakeri, K., Miryousefi Aval, S. M., Akrami, V., & Khansoltani, E. (2023). Progressive collapse analysis of intermediate moment-resisting steel frame under fire-induced column failure. Journal of Performance of Constructed Facilities, 37(4), 04023034.

[10] Miryousefi Aval, S. M., Shakeri, K., & Akrami, V. (2025). Effect of design parameters on the fire resistance of multi-story steel moment resisting frames. Steel and Composite Structures, 55(3), 273.

[11] Behnam, B. (2023). Assessment of steel structures designed for progressive collapse under localized fires. Steel and Composite Structures, 46(2), 279-292.

[12] Zhou, M., Jiang, L., Chen, S., Cardoso, R. P., & Usmani, A. (2020). Remaining fire resistance of steel frames following a moderate earthquake–A case study. Journal of Constructional Steel Research, 164, 105754.

[13] Erfani, A., & Dehestani, M. (2021). Fire resistance behavior of damaged steel portal frame with RBS connections. Journal of Constructional Steel Research, 182, 106698.

[14] Risco, G. V., Zania, V., & Giuliani, L. (2023). Numerical assessment of post-earthquake fire response of steel buildings. Safety Science, 157, 105921.

[15] Khorasani, N. E., Gernay, T., & Garlock, M. (2016). Probabilistic measures of earthquake effects on fire performance of tall buildings. In Insights and Innovations in Structural Engineering, Mechanics and Computation (pp. 1744-1749).

[16] Dashti, S., Caglayan, B. O., & Dashti, N. (2025). Post-Earthquake Fire Resistance in Structures: A Review of Current Research and Future Directions. Applied Sciences, 15(6), 3311.

[17] Suwondo, R., Cunningham, L., Gillie, M., & Bailey, C. (2019). Progressive collapse analysis of composite steel frames subject to fire following earthquake. Fire safety journal, 103, 49-58.

[18] Alasiri, M. R., Chicchi, R., & Varma, A. H. (2021). Post-earthquake fire behavior and performance-based fire design of steel moment frame buildings. Journal of Constructional Steel Research, 177, 106442.

[19] Alisawi, A. T., Collins, P. E., & Cashell, K. A. (2021). Nonlinear analysis of a steel frame structure exposed to post-earthquake fire. Fire, 4(4), 73.

[20] Gernay, T., Elhami Khorasani, N., & Garlock, M. (2015). Fragility analysis of a steel building in fire. In The First

International Conference on Structural Safety under Fire & Blast. ASRANet Ltd.

[21] Gernay, T., Khorasani, N. E., & Garlock, M. (2019). Fire fragility functions for steel frame buildings: sensitivity analysis and reliability framework. Fire Technology, 55(4), 1175-1210.

[22] Hosseini Lavasani, H., & Mahdipour, M. (2023). Vibration-based damage detection of buildings using a decision-tree-based algorithm. Numerical Methods in Civil Engineering, 8(2), 70-79.

[23] Abambres, M., Rajana, K., Tsavdaridis, K. D., & Ribeiro, T. P. (2018). Neural Network-based formula for the buckling load prediction of I-section cellular steel beams. Computers, 8(1).

[24] Kürüm Varolgüneş, F., & Varolgüneş, S. (2025). Post-Earthquake Fires (PEFs) in the Built Environment: A Systematic and Thematic Review of Structural Risk, Urban Impact, and Resilience Strategies. Fire, 8(6), 233.

[25] Sabori Ghomi, S., Shiravand, S., Zare Zardeyni, M. M., & Rabiee, N. (2025). Application of Artificial Neural Networks for Developing Temperature-Dependent Fragility Curves for Vulnerability Assessment of I-Girder Bridges. Numerical Methods in Civil Engineering, 9(4), 24-40.

[26] Fu, F. (2020). Fire induced progressive collapse potential assessment of steel framed buildings using machine learning. Journal of Constructional Steel Research, 166, 105918.

[27] Ye, Z., & Hsu, S. C. (2022). Predicting real-time deformation of structure in fire using machine learning with CFD and FEM. Automation in Construction, 143, 104574.

[28] Zhu, Y. F., Yao, Y., Huang, Y., Chen, C. H., Zhang, H. Y., & Huang, Z. (2022). Machine learning applications for assessment of dynamic progressive collapse of steel moment frames. Structures, 36, pp. 927-934.

[29] Harati, M., & van de Lindt, J. W. (2025). Machine Learning Synthesis of Fire-Following-Earthquake Fragility Surfaces for Steel Moment-Resisting Frames. Infrastructures, 10(11), 280.

[30] Behnam, B., & Abolghasemi, S. (2021). Post-earthquake fire performance of a generic fireproofed steel moment resisting structure. Journal of Earthquake Engineering, 25(13), 2579-2604.

[31] DS Simulia Corp. (2018). ABAQUS analysis user's manual. Dassault Systemes (DS) Simulia Corp. RI.

[32] Eurocode 3 (2005). Design of steel structures - Part 1-2: General rules - Structural fire design, EN 1993-1-2, Brussels, Belgium.

[33] Memari, M., Mahmoud, H., & Ellingwood, B. (2014). Post-earthquake fire performance of moment resisting frames with reduced beam section connections. Journal of Constructional Steel Research, 103, 215-229.

[34] ISO-834-1 (1999). Fire-resistance Tests -Elements of building construction. Part 1: General Requirements.

[35] Robert, A. and P. Schaumann (1986). Structural steel and plane frame assemblies under fire action. Fire Safety Journal, 10(3): 173-184.

[36] Jiang, B., G.-Q. Li and A. Usmani (2015). Progressive collapse mechanisms investigation of planar steel moment frames under localized fire. Journal of Constructional Steel Research 115: 160-168.